



Application of a Hybrid Variational Multiscale Model to Massively Separated Flows

Emmanuelle Itam, Stephen Wornom, Bruno Koobus, Alain Dervieux

► To cite this version:

Emmanuelle Itam, Stephen Wornom, Bruno Koobus, Alain Dervieux. Application of a Hybrid Variational Multiscale Model to Massively Separated Flows. AERO 2015 - 50th 3AF International Conference on Applied Aerodynamics, Mar 2015, Toulouse, France. pp.1-7. hal-01256081

HAL Id: hal-01256081

<https://inria.hal.science/hal-01256081>

Submitted on 14 Jan 2016

HAL is a multi-disciplinary open access archive for the deposit and dissemination of scientific research documents, whether they are published or not. The documents may come from teaching and research institutions in France or abroad, or from public or private research centers.

L'archive ouverte pluridisciplinaire **HAL**, est destinée au dépôt et à la diffusion de documents scientifiques de niveau recherche, publiés ou non, émanant des établissements d'enseignement et de recherche français ou étrangers, des laboratoires publics ou privés.

APPLICATION OF A HYBRID VARIATIONAL MULTISCALE MODEL TO MASSIVELY SEPARATED FLOWS

Emmanuelle Itam¹, Stephen Wornom², Bruno Koobus³, Alain Dervieux⁴

¹ I3M, Université Montpellier 2, Montpellier, France, itamemmanuelle@gmail.com, koobus@math.univ-montp2.fr

² LEMMA, 2000 route des Lucioles, Sophia-Antipolis, France, stephen.wornom@inria.fr

³ I3M, Université Montpellier 2, Montpellier, France, itamemmanuelle@gmail.com, koobus@math.univ-montp2.fr

⁴ Corresponding Author. INRIA, 2004 Route des Lucioles, F-06902 Sophia-Antipolis, Tel.: +33 4 92 38 77 91, E-mail: Alain.Dervieux@inria.fr

ABSTRACT

The simulation of high-Reynolds number massively separated flows is a challenging problem of prime interest in industry. Even in this context we have to investigate numerical tools which are able to work in a Large Eddy Simulation mode as well as RANS or the hybrid RANS-LES mode. It is then necessary to use an adapted numerical technology: in the present work, the spatial discretization is based on a mixed finite element/finite volume formulation on unstructured grids. The numerical dissipation of the upwind scheme is made of sixth-order space derivatives and corresponds to a fifth-order term in truncation error, in order to limit as far as possible the interactions between numerical and subgrid scale (SGS) dissipation, [1]. The turbulence model is based on a hybridization strategy which blends a variational multiscale large-eddy simulation (VMS-LES) equipped with dynamic SGS models and a two-equation RANS model. Particular attention is paid to the VMS-LES approach used in this work. The separation between the large and the small resolved scales is obtained through a variational projection operator based on spatial average on agglomerated cells [2]. The dynamic procedure (Germano) allows the adaptation of the constant of the SGS model to the spatial and temporal variation of the flow characteristics, while the VMS formulation restricts the SGS model effects to the smallest resolved scales [3]. The hybridization strategy uses a blending parameter, such that a VMS-LES simulation is applied in region where the grid resolution is sufficiently fine to resolve a significant part of the turbulence fluctuations, while a RANS model is used in the regions of coarse grid resolution [4]. For

instance, near the body surface, it is used under two forms, either as a statistical model for the turbulent boundary layer or as a (thinner) wall law for the LES part of the flow. The capability of the proposed hybrid model to accurately predict the aerodynamic forces acting on a circular cylinder in the supercritical regime and tandem cylinders is investigated. It is shown that rather coarse grids can be used to obtain a reasonable prediction of important bulk coefficients.

Keywords: LES, hybrid, dynamic, VMS, blunt body, cylinder, tandem

1. INTRODUCTION AND MOTIVATIONS

This work takes place in a study of numerical simulations adapted to industrial problems equipped with turbulence models suited to the simulation of turbulent flows with massive separations and vortex shedding. Recent publications concerning this study can be found in [3, 4]. The numerical methods are of low order, applicable on unstructured tetrahedrizations, and involve numerical dissipation. The dissipation is made of sixth-order derivatives, and advective accuracy can be as high as fifth order on Cartesian region of the mesh. The main issue which then arises is the choice of turbulence modelling which can be combined with this numerical technology.

In order to address high Reynolds numbers, we have to consider RANS-LES hybridization as in Detached Eddy Simulation (DES) [5, 6]. However, DES is not designed for computing subcritical flows for which pure LES is a natural approach. Therefore, it is important to have a LES mode as accurate as possible. For example, the shear layer between main flow and wake can suffer from the tendency of a

Smagorinsky-like model to apply a too strong filtering in these regions. Two devices are considered to improve the accuracy of the LES component. First, the time-space strength of the filter is controlled by a dynamic process. Second, the width of the filter is numerically controlled by using a variational multiscale formulation.

The present work focuses on the following items:

- The evaluation of dynamic and hybrid VMS-LES models on the prediction of vortex shedding flows
- The simulation of the flow around circular and tandem cylinders : these flows involve many features and difficulties encountered in industrial problems and have been studied with well documented benchmarks. They are also the first step before the computation of array of cylinders (off-shore oil and gas industries, civil engineering, aeronautics)

2. NUMERICAL MODEL : MIXED-ELEMENT-VOLUME METHOD

The spatial discretization uses a mixed finite-volume finite-element formulation, with degrees of freedom located at nodes i of the tetrahedrization. The finite volume part is integrated on a dual mesh built from medians in 2D (Figure 1) and median plans in 3D. The diffusive fluxes are evaluated by a finite-

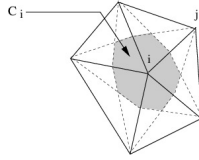


Figure 1. Dual cell in 2D

element method, the convective fluxes by a finite-volume method, with a sixth-order dissipation. Time integration is performed by an implicit second-order backward difference scheme, allowing to address flows at various Mach numbers.

3. TURBULENCE MODELING: VMS-LES

Let us explain our VMS-LES approach in a simplified context. Assume the mesh is made of two meshes embedded, corresponding to a P^1 -continuous finite-element approximation space V_h with the usual basis functions Φ_i vanishing on all vertices but vertex i . Let be V_{2h} its embedded coarse subspace V_{2h} . Let V'_h be the complementary space: $V_h = V_{2h} \oplus V'_h$. The space of *small scales* V'_h is spanned by only the fine basis functions Φ'_i related to vertices which are not vertices of V_{2h} . We write the compressible Navier-Stokes equations as follows: $\frac{\partial W}{\partial t} + \nabla \cdot F(W) = 0$ where $W = {}^t(\rho, \rho u, \rho v, \rho w, \rho E)$

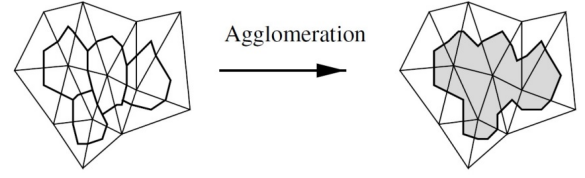


Figure 2. Building the VMS coarse level

is the set of usual conserved variables (density, moments, total energy). The VMS-LES discretization writes for a $W_h = \sum W_i \Phi_i$:

$$\left(\frac{\partial W_h}{\partial t}, \Phi_i \right) + (\nabla \cdot F(W_h), \Phi_i) = - \left(\tau^{LES}(W'_h), \Phi'_i \right)$$

In practise, embedding two unstructured meshes V_h and V_{2h} is a constraint that one wishes to avoid. The coarse level is then built from the agglomeration of vertices/cells as sketched in Figure 2. It remains to define the model term $\tau^{LES}(W'_h)$. This term represents the SGS viscosity term, acting only on small scales W'_h , and computed from the small scale component of the flow field by applying either a Smagorinsky or a WALE SGS model, the constants of these models being eventually estimated by the Germano-Lilly dynamic procedure.

The main property of the VMS formulation is that the modeling of the unresolved structures is influencing only the small resolved scales, in contrast with, for example, the usual Smagorinsky model. This implies two main properties. First, the backscatter transfer of energy to large scales is not damped by the model. Second, the model does not produce an artificial viscous layer at no-slip boundaries, nor in shear layers.

4. TURBULENCE MODELING: HYBRID RANS/VMS-LES

The computation of massively separated flows at high Reynolds number on unstructured mesh can be addressed with three families of models. RANS is robust but lacks accuracy in flow regions with massive separation (as the flow around bluff-bodies). LES, and in particular our VMS-LES is more expensive than RANS, since a very fine resolution - comparable to DNS- is required in boundary layers at high Reynolds number. Hybrid formulations combine RANS and LES in order to exploit the advantages of the two approaches. Our goal is to build and evaluate a hybrid RANS/VMS-LES. The central idea of the proposed hybrid VMS model is to correct the mean flow field obtained with a RANS model by adding fluctuations given by a VMS-LES approach wherever the grid resolution is adequate. In the above simplified case it writes:

$$\left(\frac{\partial W_h}{\partial t}, \Phi_i \right) + (\nabla \cdot F(W_h), \Phi_i) = \theta \left(\tau^{RANS}(\langle W \rangle), \Phi_i \right) - (1 - \theta) \left(\tau^{LES}(W'_h), \Phi'_i \right)$$

where the blending function $\theta = \tanh(\xi^2)$ is defined either by a prescription of the user (zonal option) or from $\xi = \mu_{SGS}/\mu_{RANS}$ or $\xi = \Delta/l_{RANS}$, allowing to have most regions with $\theta = 0$, VMS-LES, or $\theta = 1$, RANS. The RANS is a $k-\varepsilon$ proposed by Goldberg *et al.* in [7].

This model relies on a unique damping function

$$\mu_t = C_\mu f_\mu \rho \frac{k^2}{\varepsilon} ; f_\mu = \frac{1 - e^{-A_\mu R_t}}{1 - e^{-R_t^{1/2}}} \max(1, \psi^{-1})$$

with $C_\mu = 0.09$, $A_\mu = 0.01$, and where $\psi = R_t^{1/2}/C_\tau$, $R_t = k^2/(\nu\varepsilon)$ is a turbulent Reynolds number. The transport equations become:

$$\left\{ \begin{array}{l} \frac{\partial \bar{\rho}k}{\partial t} + \frac{\partial(\bar{\rho}\hat{u}_j k)}{\partial x_j} = \frac{\partial \left[\left(\mu + \frac{\rho\mu}{\sigma_k} \right) \frac{\partial k}{\partial x_j} \right]}{\partial x_j} + R_{ij} \frac{\partial \hat{u}_i}{\partial x_j} - \bar{\rho}\varepsilon, \\ \frac{\partial \bar{\rho}\varepsilon}{\partial t} + \frac{\partial(\bar{\rho}\hat{u}_j \varepsilon)}{\partial x_j} = \frac{\partial \left[\left(\mu + \frac{\rho\mu}{\sigma_\varepsilon} \right) \frac{\partial \varepsilon}{\partial x_j} \right]}{\partial x_j} + \left(C_{\varepsilon 1} R_{ij} \frac{\partial \hat{u}_i}{\partial x_j} - C_{\varepsilon 2} \bar{\rho}\varepsilon + E_\tau \right) T_\tau^{-1} \end{array} \right.$$

where $-$ and \sim denote the Reynolds and Favre average respectively. In the above equations, T_τ , representing the realizable time scale, and the extra term E_τ are defined by:

$$T_\tau = \frac{k}{\varepsilon} \max(1, \psi^{-1}) ; E_\tau = \rho A_E V (\varepsilon T_\tau)^{0.5} \xi.$$

For our applications, we keep the constants proposed in [7]:

$$C_\tau = 1.41 \quad C_{\varepsilon 1} = 1.42 \quad C_{\varepsilon 2} = 1.83$$

and the extra term E_τ is computed with: $A_E = 0.3$, $V = \max(\sqrt{k}, (\nu\varepsilon)^{0.25})$ and $\xi = \max(\frac{\partial k}{\partial x_i} \frac{\partial \tau}{\partial x_i}, 0)$, where $\tau = k/\varepsilon$. The interest of this model is its ability to detect the near-wall region without using a distance-to-wall, an important advantage when our unstructured-mesh method is applied to complex geometries. Furthermore, this model is well suited to the simulation of adverse pressure gradient flows, and in particular when flow separation occurs.

5. WALL TREATMENT

The title of this section could also be the title of the previous one since today's use of hybrid models is mainly concentrated on the boundary layers. But some other issues need to be discussed for wall treatment (WT). First, we need to identify which kind of boundary behavior appears in the family of flow studied here.

First, we can distinguish at least three types of behavior and then three combinations:

(a)- Laminar WT of LES for subcritical flow regime: the upstream flow is not turbulent and the boundary layer remains laminar, the turbulence being limited to a part of the wake at some distance from the body. This is the situation of subcritical flows around smooth bodies like circular cylinders.

(b)- Turbulent wall modeling for LES: the upstream flow is turbulent, with a high Reynolds number, but can be represented -far from wall- by an (unsteady) LES model. This is the wall-modeled LES (WMLES), see [8]. In this case, a wall law can be applied as far as only a part of the usual model is used, typically for y^+ less than 40.

(c)- Fully turbulent WT for supercritical flows: typically, the upstream flow is not turbulent, but the boundary layer has transitioned and becomes fully turbulent. The RANS, with or without wall law, needs to be used with y^+ more than 40.

Further, a fully predictive model should involve the modeling of the switching from one WT to another one:

- (a')** Laminar to fully turbulent
- (b')** Fully turbulent to WMLES
- (c')** Relaminarisation.

We do not address in the present paper the problem of the prediction of these switchings. For (c'), a discussion can be found in [9].

As concerned the WT itself, and from the standpoint of prediction accuracy, resolution to the wall is compulsory for the study of flows around blunt bodies, but still too computer intensive for the study of industrial geometries like risers with thousands-diameter span.

In the present study, we have applied the following rule-of-thumb:

Wall law modeling will relies on the Reichardt formula, [10]. The interest of this model is to describe, through one expression, the three types of behavior of the turbulent boundary layer, viz, the laminar layer, the logarithmic one and the intermediate (buffer) layer.

$$U^+ = \frac{1}{\kappa} \ln(1 + \kappa y^+) + 7.8 \left(1 - e^{-\frac{y^+}{11}} - \frac{y^+}{11} e^{-0.33y^+} \right)$$

with:

$$U_\tau = \sqrt{\frac{\tau_p}{\rho}} ; U^+ = \frac{\bar{U}}{U_\tau} ; y^+ = \frac{\rho U_\tau y}{\mu}$$

in which \bar{U} , ρ , μ and y are averaged tangential velocity, density, molecular viscosity and normal distance to the wall respectively, and U_τ denotes the friction velocity.

For (a) this choice is delicate. It can be applied for y^+ less than 20. For (b), it can be used for y^+ less than 40. For (c) the wall law will be used with matching inside the logarithmic part, y^+ more than 40.

Resolution to the wall for (a),(b),(c) will similarly be applied by choosing a mesh with first layer of points corresponding to $y^+ = 1$, and defining near the wall several thickness corresponding to several "protection zones" for the hybrid model:

For (a) by either forcing the hybrid blending parameter to 1 for y^+ less than 20, or preferably computing the boundary layer as laminar.

For (b) by forcing the hybrid blending parameter to 1 for y^+ less than 40.

For (c) by forcing the hybrid blending parameter to 1 for y^+ less than 200.

6. APPLICATIONS : CIRCULAR CYLINDER - SUBCRITICAL REGIME

The flow around a cylinder is strongly dependant on the turbulence which exists in the inflow and the turbulence which is created along the wall boundary layer after the stagnation point. In case where the inflow involves no turbulence, turbulence is created on the wall for a sufficiently high critical Reynolds number, corresponding to the *drag crisis*. This Reynolds number is between 300,000 and 500,000. Under this number, the flow is subcritical and, in short the boundary layer flow is laminar. In this case, we put $\theta = 0$ in our model, which means that the VMS-LES model is combined with a laminar boundary layer, an option which is justified when the turbulence arising is essentially wake turbulence.

We choose here a rather low Reynolds of 3900 (Mach number is 0.1) and analyse in which conditions a better prediction is obtained with a very coarse mesh (290,000 vertices) and a medium mesh (1,400,000 vertices). The WALE SGS model is used, and we compare the association of VMS-WALE with dynamic limitation and without. Surprisingly, the effect on wake velocity is small in general, but yet rather notable at the limit of the wake, see Figures 3. For a higher Reynolds of 20,000, we observed that the effect of the dynamic procedure is rather determinant for the proper prediction of the turbulent intensity in the wake, particularly in VMS, see Figure 4. Global coefficient are also slightly improved, see Table 1 where our results are compared with some LES computations [11, 12, 13] and measurements data [13, 14, 15].

7. CIRCULAR CYLINDER - SUPERCRITICAL REGIME

We address now the flow around a circular cylinder at a Reynolds of 1 million, higher than the critical one. We propose to compare the results of three options, (a) $\theta = 0$, that is RANS, (b) $\theta = 1$, that is VMS-WALE, (c) hybrid RANS/VMS-WALE. Moreover, we try to get reasonable results with a medium-sized mesh of 1.2 million vertices. The available experiments are not so many, [16, 17, 18], and show some scatter. Computations are also difficult to find in the litterature, we have found [19, 20, 21], which present a higher scatter and deviation to measurements (Table 2). Among options (a),(b),(c), we observe that the hybrid calculation is in a rather good accordance with the measurements. A snapshot of the vorticity field computed by the hybrid model is depicted in Figure 5, which shows that rather fine details of the flow are still captured with the medium-sized mesh used in our simulation.

	Mesh	\bar{C}_d	l_r/D	$-\bar{C}_{p_b}$	St
VMS	270K	0.96	1.06	0.94	0.22
VMS dyn.	270K	0.97	1.08	0.93	0.22
VMS	1.4M	0.94	1.47	0.81	0.22
VMS dyn.	1.4M	0.94	1.47	0.85	0.22
LES					
Lee(Min)	7.7M	0.99	1.35	0.89	0.209
Lee(Max)	7.7M	1.04	1.37	0.94	0.212
Kravchenko					
(Min)	0.5	1.04	1.	0.93	0.193
(Max)	2.4M	1.38	1.35	1.23	0.21
Parneadeau					
(Min)	44M	-	1.56	-	0.207
(Max)	44M	-	1.56	-	0.209
Experiments					
Parneadeau					
(Min)		-	1.51	-	0.206
(Max)		-	1.51	-	0.210
Norberg					
(Min)		0.94	-	0.83	
(Max)		1.04	-	0.93	
Ong(Min)		-	-	-	0.205
Ong(Max)		-	-	-	0.215

Table 1. Bulk quantities for Re=3900 flow around a cylinder (VMS-WALE vs VMS-WALE dynamic)

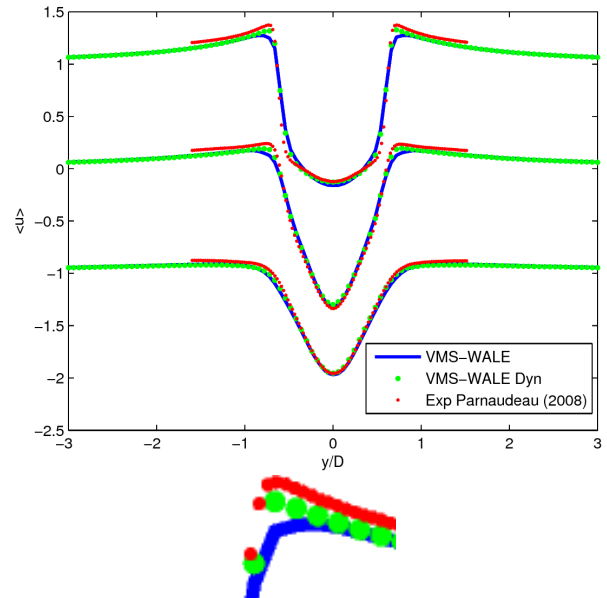


Figure 3. Cylinder, Re=3900: Mean streamwise velocity profile at $x/D = 1.06$, 1.54 and 2.02 and a zoom of the $x/D = 1.06$ cut (finer grid).

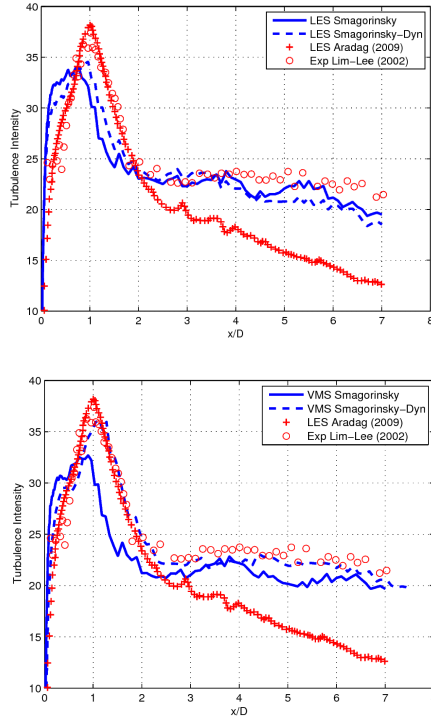


Figure 4. Cylinder, $Re=20,000$: turbulence intensity in the axis of wake: Dynamic improves LES (top) and strongly improves VMS (bottom).

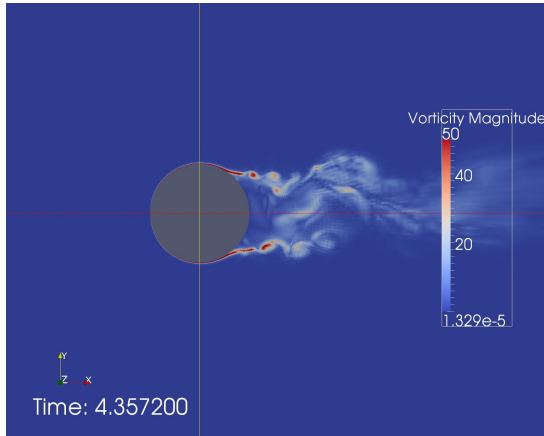


Figure 5. Flow around a circular cylinder at $Re=1$ million: vorticity field computed by the hybrid RANS/VMS-LES model.

	Mesh	\bar{C}_d	C'_l	$-\bar{C}_{p_b}$	St
URANS	1.2M	0.24	0.06	0.25	0.46
VMS WALE	1.2M	0.36	0.22	0.22	0.10
Hybrid:					
VMS-WALE	1.2M	0.24	0.17	0.28	0.17
Catalano:					
URANS	2.3M	0.40	-	0.41	0.31
LES	2.3M	0.31	-	0.32	0.35
LES Kim	6.8M	0.27	0.12	0.28	-
Exp.:					
Shih		0.24	-	0.33	-
Gölling		-	-	-	0.10
Zdravkovich:					
(Min)		0.2	0.1	0.2	0.18
(Max)		0.4	0.15	0.34	0.18

Table 2. Flow around a circular cylinder at $Re=1$ million: bulk coefficients.

8. TANDEM CYLINDER

The last case concerns the flow around two cylinder in tandem, at $Re=1.66 \times 10^5$. This is a test case studied in an AIAA workshop, see [22]. Among the conclusions of the workshop, addressing this case with LES was considered as a too difficult task with existing computers. Results with DES were much closer to measurements. We have computed the case with a mesh of 2.59 million nodes. Two modeling options were considered: (a) RANS and (b) Hybrid VMS-LES-WALE dynamic. An idea of the impact of these options on the resulting flow is proposed in Figure 6, where an excessive damping of the flow is observed for the RANS computation. Some comparison of bulk coefficients is given in Table 3 in which the other computational figures are taken from [23] and for Lockard and Aybay from [22]. The experimental drag values were obtained by integrating outputs found in [24]. Drag for the first cylinder shows a small scatter with the various hybrid calculations.

In a first hybrid computation, with wall law, option (c), thick turbulent boundary layer has been applied to the two cylinders. Pressure distribution is shown in Figure 7.

In a second hybrid simulation, integration to the wall is used. The thick turbulent boundary layer is restricted to the front part of the first cylinder. Option (b) is applied to the rest of cylinder 1 wall. Cylinder 2 is not equipped with a protection zone. The simulation around the second cylinder is more challenging as also illustrated by the pressure distributions (Figure 8).

	Mesh	\bar{C}_d Cyl. 1	\bar{C}_d Cyl. 2
Hybrid VMS dyn.	2.59M	0.64	0.38
Numerical results			
Lockard (2011)	2M-133M	0.33-0.80	0.29-0.52
DES Aybay (2010)	6.7M	0.64	0.44
HRLES Vatsa (2010)	8.7M	0.64	0.45
Experiments			
Neuhart et al. (2009)		0.64	0.31

Table 3. Tandem of cylinders: bulk coefficients.

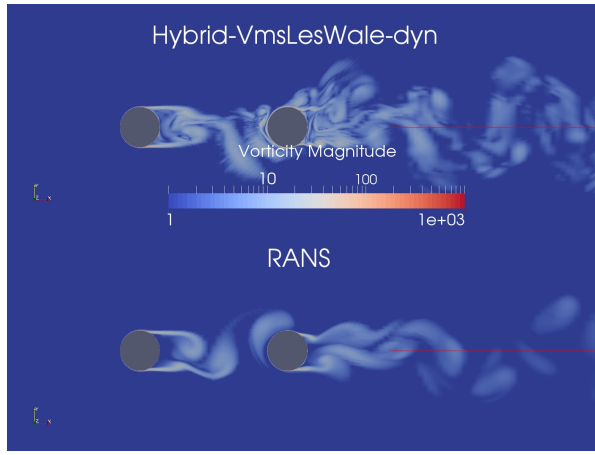


Figure 6. Tandem of cylinders: Vorticity magnitude - Hybrid VMS versus RANS.

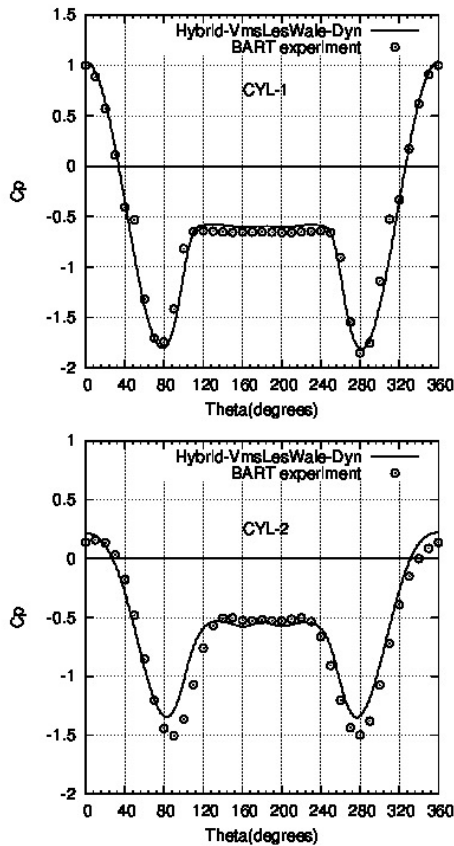


Figure 7. Tandem of cylinders with wall law and hybrid model: Mean pressure coefficient distribution.

9. CONCLUSION, PERSPECTIVES

The main effect of dynamic control of SGS is a significant reduction of the amount of SGS viscosity in VMS-LES. The impact is in VMS-LES smaller than for pure LES but still non-negligible. In a large part of the tested cases we observe that the dynamic procedure brings a sensible improvement of the agreement with reference data. Then we have presented a strategy for blending RANS and VMS-LES. The supercrit-

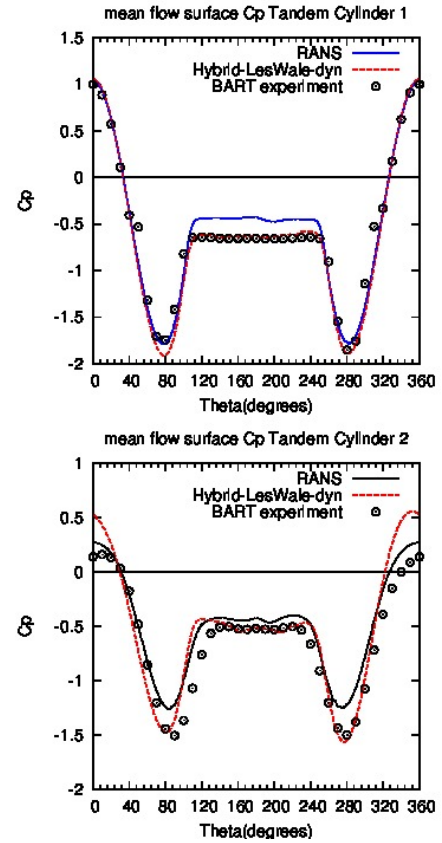


Figure 8. Tandem of cylinders with integration to wall: Mean pressure coefficient distribution.

ical flow around a circular cylinder is reasonably well predicted by the proposed VMS hybrid model. The tandem cylinder case shows at the same time some improvement and that further research is necessary.

10. ACKNOWLEDGEMENTS

This work has been supported by French National Research Agency (ANR) through project MAID-ESC n° ANR-13-MONU-0010. HPC resources from GENCI-[CINES] (Grant 2010-x2010026386 and 2010-c2009025067) are also gratefully acknowledged.

REFERENCES

- [1] Camarri, S., Koobus, B., Salvetti, M. V., and Dervieux, A., 2004, "A low-diffusion MUSCL scheme for LES on unstructured grids", *Computer and Fluids*, Vol. 33, pp. 1101–1129.
- [2] Koobus, B., and Farhat, C., 2004, "A variational multiscale method for the large eddy simulation of compressible turbulent flows on unstructured meshes-application to vortex shedding", *Comput Methods Appl Mech Eng*, Vol. 193, pp. 1367–1383.
- [3] Moussaed, C., Wornom, S., Salvetti, M., Koobus, B., and Dervieux, A., 2014, "Impact of dynamic subgrid-scale modeling in variational

- multiscale large-eddy simulation of bluff body flows", *Acta Mechanica*, Vol. 225, pp. 3309–3323.
- [4] Moussaed, C., Salvetti, M., Wornom, S., Koobus, B., and Dervieux, A., 2014, "Simulation of the flow past a circular cylinder in the supercritical regime by blending RANS and variational-multiscale LES models", *Journal of Fluids and Structures*, Vol. 47, pp. 114–123.
 - [5] Spalart, P., Jou, W.-H., Strelets, M., and Allmaras, S., 1997, "Comments on the feasibility of LES for wings, and on a hybrid RANS/LES approach", C. Liu, and Z. Liu (eds.), *Advances in DES/LES*, 1 st AFOESR Int. Conf. On DNS/LES,(1997), Ruston, LA, Greyden Press, Columbus, OH, pp. 137–147.
 - [6] Spalart, P., Deck, S., Strelets, M., Shur, M., Travin, A., and Squires, K., 2006, "A new version of detached-eddy simulation, resistant to ambiguous grid densities", *Theor Comput Fluid Dyn*, Vol. 20, pp. 181–195.
 - [7] Goldberg, U., Perroomian, O., and Chakravarthy, S., 1998, "A wall-distance-free $k - \varepsilon$ model with Enhanced Near-Wall Treatment", *Journal of Fluids Engineering*, Vol. 120, pp. 457–462.
 - [8] Piomelli, U., and Balaras, E., 2002, "Wall-layer models for Large-Eddy Simulations", *Annual Review of Fluid Mechanics*, Vol. 34, pp. 349–374.
 - [9] Shur, M., Spalart, P., Strelets, M., and Travin, A., 2008, "A hybrid RANS-LES approach with delayed-DES and wall-modelled LES capabilities", *International Journal of Heat and Fluid Flow*, Vol. 29, p. 1638 1649.
 - [10] Reichardt, H., 1951, "Vollstaendige Darstellung der turbulenten Geschwindigkeitsverteilung in glatten Leitungen", *Zeitschrift fuer Angewandte Mathematik und Mechanik*, Vol. 31, p. 208.
 - [11] Lee, J., Park, N., Lee, S., and Choi, H., 2006, "A dynamical subgrid-scale eddy viscosity model with a global model coefficient", *Phys Fluids*, Vol. 18 (12), p. 125109.
 - [12] Kravchenko, A., and Moin, P., 1999, "Numerical studies of flow over a circular cylinder at $Re=3900$ ", *Phys Fluids*, Vol. 12 (2), pp. 403–417.
 - [13] Parnaudeau, P., Carlier, J., Heitz, D., and Lamballais, E., 2008, "Experimental and numerical studies of the flow over a circular cylinder at Reynolds number 3900", *Phys Fluids*, Vol. 20 (8), p. 085101.
 - [14] Norberg, C., 1987, "Effects of Reynolds number and low-intensity free-stream turbulence on the flow around a circular cylinder", *Tech. Rep. 87/2*, Department of Applied Thermosc. and Fluid Mech., Chalmers University of Technology, Gothenburg, Sweden.
 - [15] Ong, L., and Wallace, J., 1996, "The velocity field of the turbulent very near wake of a circular cylinder", *Exp Fluids*, Vol. 20, pp. 441–453.
 - [16] Shih, W., Wang, C., Coles, D., and Roshko, A., 1993, "Experiments on flow past rough circular cylinders at large Reynolds numbers", *J Wind Eng Indust Aerodyn*, Vol. 49, pp. 351–368.
 - [17] Gölling, B., 2006, "Experimental investigations of separating boundary-layer flow from circular cylinder at Reynolds numbers from 10^5 up to 10^7 ; Three-dimensional vortex flow of a circular cylinder", G. Meier, and K. Sreenivasan (eds.), *Proceedings of IUTAM Symposium on One Hundred Years of Boundary Layer Research*, Springer, The Netherlands, pp. 455–462.
 - [18] Zdravkovich, M., 1997, *Flow around circular cylinders Vol 1: Fundamentals.*, Oxford University Press.
 - [19] Wang, M., Catalano, P., and Iaccarino, G., 2001, "Prediction of high Reynolds number the flow over a circular cylinder using LES", *Annual research briefs*, Center for Turbulence Research, Stanford.
 - [20] Catalano, L., 2002, "A new reconstruction scheme for the computation of inviscid compressible flows on 3D unstructured grids", *International Journal for Numerical Methods in Fluids*, Vol. 40 (1-2), pp. 273–279.
 - [21] Kim, S.-E., and Mohan, L., 2005, "Prediction of unsteady loading on a circular cylinder in high Reynolds number flows using large eddy simulation", *Proceedings of OMAE 2005: 24th International Conference on Offshore Mechanics and Artic Engineering*, June 12-16, OMAE 2005-67044, American Society of Mechanical Engineers, Halkidiki, Greece.
 - [22] Lockard, D., 2011, "Summary of the Tandem Cylinder Solutions from the Benchmark Problems for Airframe Noise Computations-I", *Proceedings of 49th AIAA Aerospace Sciences Meeting*, AIAA-2011-353, Orlando, Florida.
 - [23] Vatsa, V., and Lockard, D., 2010, "Assessment of Hybrid RANS/LES turbulence models for aeroacoustics applications", *AIAA Paper*, AIAA-2010-4001.
 - [24] Neuhaert, D., Jenkins, L., Choudhari, M., and Khorrami, M., 2009, "Measurements of the flowfield interaction between tandem cylinders", *AIAA Paper*, AIAA-2009-3275.